Hydrological modelling of stalagmite δ18O response to glacial-interglacial transitions

Author:
Baker, A; Bradley, C; Phipps, Steven

Publication details:
Geophysical Research Letters
v. 40
Chapter No. 12
pp. 3207-3212
0094-8276 (ISSN)

Publication Date:
2013

Publisher DOI:
http://dx.doi.org/10.1002/grl.50555

Hydrological modeling of stalagmite $\delta^{18}O$ response to glacial-interglacial transitions

Andy Baker,[1] Chris Bradley,[2] and Steven J. Phipps[3]

Received 23 March 2013; revised 8 May 2013; accepted 10 May 2013; published 19 June 2013.

[1] Stalagmite $\delta^{18}O$ series currently provide the most robustly dated characterization of glacial terminations. However, uncertainties associated with the stalagmite $\delta^{18}O$ proxy record arise due to the complexity of flow within karst aquifers. Here we use an integrated climate-soil-groundwater lumped parameter hydrological model to demonstrate the range of potential stalagmite $\delta^{18}O$ hydrological responses to significant global climate changes. Pseudoproxy stalagmite $\delta^{18}O$ series were generated for millennial length model simulations, using general circulation model time-slice data for 12, 11, and 10 ka for eastern China. Our model demonstrates that the variability within published $\delta^{18}O$ records from Chinese stalagmites falls within that of modeled pseudoproxy series. We utilize model output to (i) quantify hydrological uncertainty (specifically the relative importance of changing precipitation amount, isotopic composition, and water balance); (ii) identify any nonstationarity in $\delta^{18}O$ variability and its relationship to climate change; and (iii) demonstrate the processes that produce low-frequency power in stalagmite $\delta^{18}O$. **Citation:** Baker, A., C. Bradley, and S. J. Phipps (2013), Hydrological modeling of stalagmite $\delta^{18}O$ response to glacial-interglacial transitions, *Geophys. Res. Lett.*, *40*, 3207–3212, doi:10.1002/grl.50555.

1. Introduction

[2] Over millennial and longer time scales, stalagmite $\delta^{18}O$ provides a precisely datable proxy of global change [*Wang et al*., 2001, 2008; *Cheng et al*., 2009, 2012]. The primary source of speleothem $\delta^{18}O$ is precipitation, which has been investigated for modern-day East Asia [*Dayem et al*., 2010]. Precipitation is subject to evaporative fractionation in the soil and shallow epikarst. Drip-water $\delta^{18}O$ is further modified by water storage and mixing within the soil, epikarst, and karst. Finally, fractionation occurs during speleothem deposition. These processes have been quantified to varying degrees using hydrological models of mixing and storage in the karst [*Bradley et al*., 2010; *Baker et al*., 2012] and geochemical models of isotope fractionation during stalagmite deposition [*Scholz et al*., 2009].

[3] Our objective in this paper is to quantify the range of possible stalagmite $\delta^{18}O$ signatures introduced by hydrological variability over glacial to interglacial transitions. We use a lumped parameter model to generate multiple millennial length pseudoproxy simulations of stalagmite $\delta^{18}O$ across the onset of the Holocene. Using output from the Commonwealth Scientific and Industrial Research Organisation (CSIRO) Mk3L general circulation model, we model paleoclimate scenarios to derive pseudoproxy series to compare with speleothem $\delta^{18}O$. As an example, we use speleothem $\delta^{18}O$ from Hulu Cave, Nanjing, China [*Wang et al*., 2001] using data from the U.S. National Climate Data Center (http://www.ncdc.noaa.gov/paleo/). Stalagmites from this cave, situated at 35 m depth in Ordovician limestone, provide replicated records of speleothem $\delta^{18}O$ for the last glacial termination.

2. Methods

[4] We use a modified version of the karst hydrology model used by *Bradley et al*. [2010] to model stalagmite $\delta^{18}O$ (see Figure S1 in the supporting information). The model envisages five water stores: (i) Soil, (ii) Epikarst, (iii) Karst Store 1, (iv) Karst Store 2, and (v) an Overflow Store. Each store drains monthly at a rate proportional to the volume of water stored (see supporting information for code). The sole hydrological input to the model is precipitation (*P*) (to Soil Store), and outputs are evapotranspiration (*ET*) (from Soil Store) and drip-water flow within the cave and drainage. Model constraints include the following: (i) no flow occurs from the Soil Store when surface temperatures (*T*) are $<0.0^{\circ}C$; (ii) flow from the Epikarst to Karst Store 2 (*F4*) occurs when Epikarst water storage exceeds threshold *Epicap*; and (iii) flow from Karst Store 2 to the Overflow Store (*F7*) occurs when the former exceeds threshold *Ovcap*. The model assumes that fracture flow between stores is the dominant flow process, an acceptable assumption for mature limestones with low primary porosity. The model has previously been shown to produce pseudoproxy stalagmite $\delta^{18}O$ series that agree with modern stalagmite $\delta^{18}O$ for three sites (Gibraltar, NW Scotland, and Ethiopia) in *Bradley et al*. [2010].

[5] The $\delta^{18}O$ composition of each store is modeled as a function of precipitation ($\delta^{18}O_p$) and store $\delta^{18}O$ in the preceding time step, allowing for evaporative fractionation in the Soil Store. Individual drip-water $\delta^{18}O$ series are generated by assuming that drip-waters are (i) solely derived from a particular water store; (ii) the product of mixing of waters draining from a selection of water stores; and (iii) a

Additional supporting information may be found in the online version of this article.

[1]Connected Waters Initiative Research Centre and National Centre for Groundwater Research and Training, University of New South Wales, Sydney, New South Wales, Australia.
[2]School of Geography, Earth and Environmental Sciences, University of Birmingham, Birmingham, UK.
[3]Climate Change Research Centre and ARC Centre of Excellence for Climate System Science, University of New South Wales, Sydney, New South Wales, Australia.

Corresponding author: A. Baker, Connected Waters Initiative Research Centre, University of New South Wales, Sydney, Australia. (a.baker@unsw.edu.au)

0094-8276/13/10.1002/grl.50555

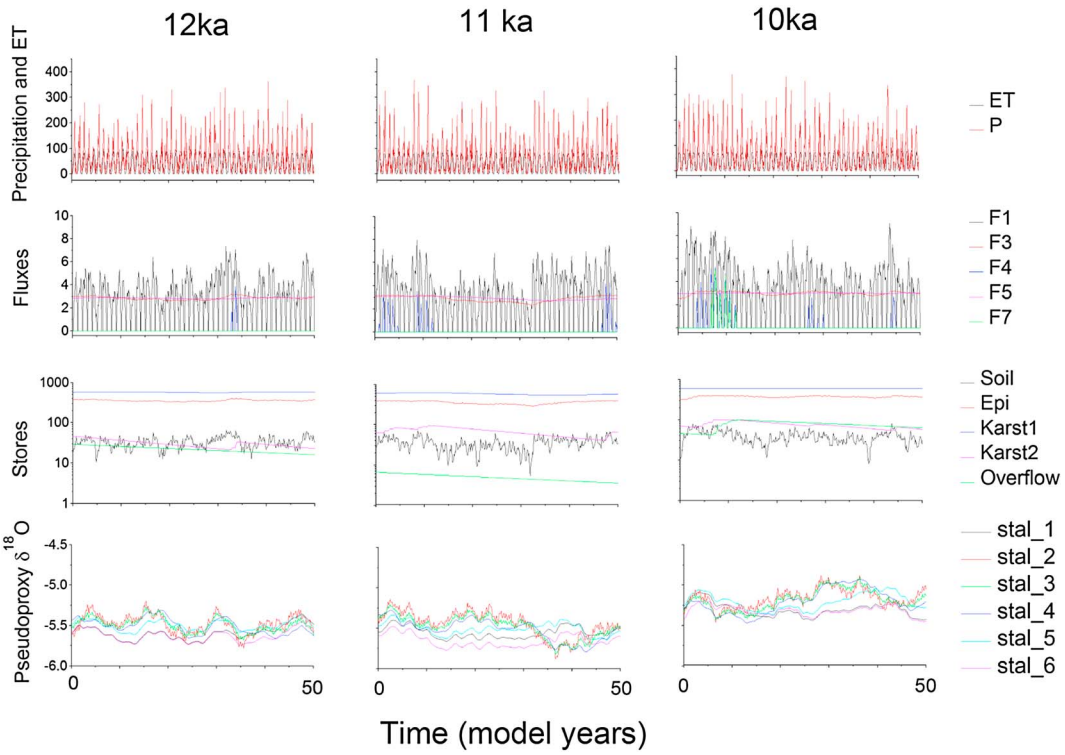

Figure 1. Comparison of glacial and postglacial model simulations, presenting arbitrary 600 month time slices at 12, 11, and 10 ka, for steady state parameters of $F3 = 0.008$, $F5 = 0.005$, and $Ovcap = 100$. Further time slices are presented in supporting information Figure S2.

combination of store drainage and recent precipitation $\delta^{18}O$ (arising through preferential flow through the soil and limestone). Stalagmite $\delta^{18}O$ series (*Stal_1* to *Stal_6*) are derived from each drip-water $\delta^{18}O$ series by allowing for calcite fractionation (we use the commonly applied method of *Kim and O'Neil* [1997], where T is the mean temperature of the preceding 12 months).

[6] As input data, we utilized 1000 year series of monthly T, P, and ET representative of the climate of Nanjing, China, for time slices 12, 11, and 10 ka, a period that encompasses the Younger Dryas event. P and T series were obtained using the CSIRO Mk3L climate system model version 1.2, a reduced-resolution atmosphere-land-sea ice-ocean general circulation model [*Phipps et al.*, 2011, 2012]. The model was integrated to equilibrium under 12, 11, and 10 ka boundary conditions but without any North Atlantic freshwater flux during the Younger Dryas. The Earth's orbital parameters were set equal to the appropriate values for each epoch, and the land ice sheets were specified according to the ICE-5G reconstruction v1.2 [*Peltier*, 2004]. The atmospheric greenhouse gas concentrations specified are shown in Table S1 in the supporting information. After reaching equilibrium, the model was integrated for a further 1000 years to generate the climatological output used in this study. Monthly potential ET was estimated following *Thornthwaite* [1948]: despite the known limitations of this method [*Chen et al.*, 2005], it is a practical approach for monthly time steps and with limited ET input parameters. For $\delta^{18}O_p$, we take the monthly mean precipitation $\delta^{18}O$ from the last glacial maximum (21 ka) general circulation modeling of *Pausata et al.* [2011], applying a 1σ variance for all months of 1.6‰ (the mean variability in the modern IAEA Nanjing GNIP data). Isotope and climate data were obtained from the International Atomic Energy Association: (http://www-naweb.iaea.org/napc/ih/index.html). Given our relatively poor knowledge of $\delta^{18}O_p$ variations from glacial to interglacial periods, $\delta^{18}O_p$ was not varied between the 12, 11, and 10 ka time-slice model simulations. A 1500 year input series was generated from the 1000 year monthly series of P, T, ET, and $\delta^{18}O_p$ by repeating 500 years of the data at the start of the series. This helped us discount model initiation effects and ensured that the karst water stores had reached their equilibrium size before the time periods presented here.

[7] In our model, the principal hydrological control on drip-water $\delta^{18}O$ is the relative size of each store in relation to water inflows and outflows. Where storage volume is large in relation to the drainage rate, $\delta^{18}O$ variability will be low and drip-water supply will be continuous, whereas a high drainage rate relative to storage volume results in high $\delta^{18}O$ variability and discontinuous outflow. Because we are comparing records for stalagmites exhibiting continuous deposition for 10^3–10^4 years, we are able to constrain the drainage function of a particular water store accordingly. A series of model runs were completed to determine the preferred parameter set (i.e., drainage functions and initial storage volumes in each store), focusing initially on parameters describing $F3$ and $F5$ followed by *Epicap* and *Ovcap*. We first varied the $F5$ drainage term systematically from 0.2 to 0.001 and identified (i) the time when the model output stabilized (i.e., $F3 \approx F5$) and (ii) the water volume in each store at this time. Final selected parameters ($F3$: 0.008; *Epicap*: 400 mm) yielded a range of steady state water stores (i.e., Epikarst Store 2 to 10 times greater than Soil Store). *Ovcap* was then defined as 100 mm, ensuring that flow to

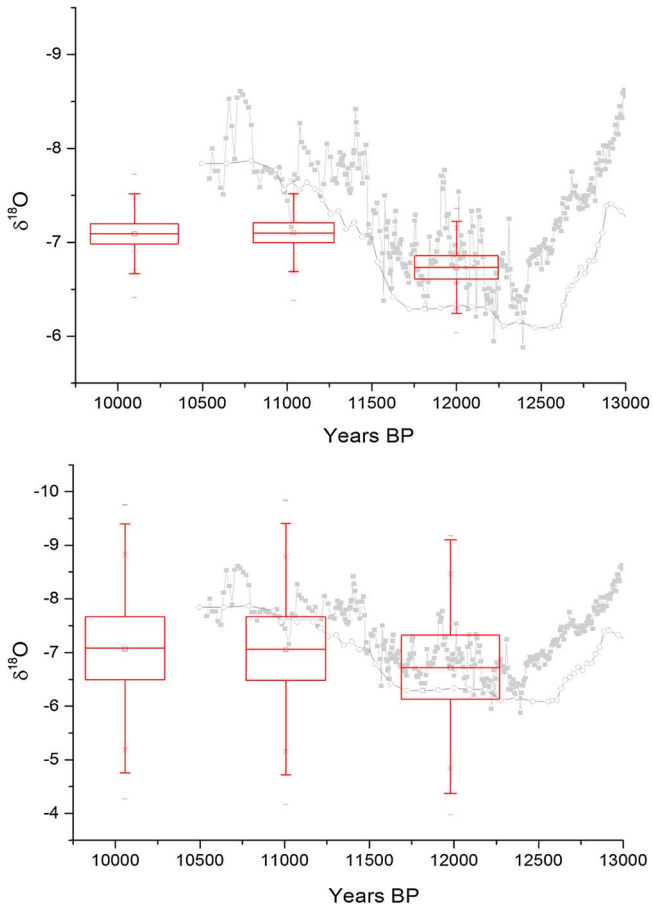

Figure 2. Comparison of model output and stalagmite data: (top) *Stal_5* (base) *Stal_3*. Model output is offset by +1.5‰ to permit visual comparison with stalagmite data. Monthly resolution model output is smoothed to a 5 year average to be comparable with stalagmite series H82 (squares: mean sampling interval of 8 ± 4 years). Stalagmite PD has a mean sampling interval of 59 ± 36 years (circles). Boxplots show mean (square), 1 and 99 percentiles (cross), range (dash), and interquartile range, and are for model output for the 10 stable model configurations: $F3 = 0.0064 \rightarrow 0.0096$; $F5 = 0.004 \rightarrow 0.006$; *Ovcap* $80 \rightarrow 120$.

the Overflow Store (*F*7) occurred regularly. The steady state parameters for $F3 = 0.008$ were used to determine the optimum term for *F*5 (flow from the epikarst). For a drainage parameter of 0.005, the relative sizes of the Karst, Epikarst, and Soil Stores were preserved. If this term is too large (i.e., 0.05), then Karst Store 1 emptied quickly and was smaller in size than the Soil Store; however, if the term was too small (0.0005), very little water flowed from Karst Store 1, which became too large in size.

3. Results

[8] To demonstrate the stability of the model, we first present modeled water movement for three 50 year periods chosen arbitrarily from the 12, 11, and 10 ka 1000 year time slices (Figure 1). Further examples are provided in Figure S2 in the supporting information. Input series (*P* and *ET*); fluxes to and from the epikarst (*F*1 and *F*3); fluxes to and from Karst Store 1 (*F*3 and *F*5), Karst Store 2 (*F*1 and *F*4), and the Overflow Store (*F*7); and the water volume in each store are shown, together with six different modeled pseudoproxy stalagmite series: *Stal_1* to *Stal_6*. These are presented as 5 year smoothed data to better reflect typical stalagmite sampling resolution.

[9] The pseudoproxy series vary markedly as a result of differences in the inferred water flow path and in the extent to which drip-water isotopic composition is attenuated by mixing within water stores of varying size within the karst. Figure 1 demonstrates that there is a clear seasonal cycle in the main input series of *P* and *ET*, which accounts for the variation in *F*1 (flows to Epikarst) over time. Flow from the Epikarst (*F*3) is strongly attenuated but varies according to any changes in water storage, while there are no seasonal variations in flow from Karst Store 1. However, the volume of water stored in Karst Store 1 is ~1.5 times greater than in the Epikarst Store, and hence the model predicts a considerable range in the isotopic composition of the different stalagmite series. Little variation is found in those series fed by drip-waters from the main water stores (the Epikarst and Karst Stores 1 and 2), but where preferential flow occurs, recent $\delta^{18}O_p$ influences the stalagmite series, imparting a clear seasonal trend. Thus, the same model input series can yield a range of possible stalagmite $\delta^{18}O$ series that reflect water routing though the karst and the degree of mixing that has occurred.

[10] Figure 2 shows pseudoproxy $\delta^{18}O$ output for two representative series, *Stal_5* and *Stal_3*, shown as boxplots of results from all karst model configurations, for the 12, 11, and 10 ka time slices, compared to actual stalagmite data. Pseudoproxy data for all model output are presented in Figure S3 in the supporting information. Pseudoproxy mean $\delta^{18}O$ are 1.5‰ heavier than the stalagmite series: a mismatch in absolute isotope values between series was expected given our use of best available $\delta^{18}O_p$ data, which was from the Last Glacial Maximum, and here we only consider the relative changes in $\delta^{18}O_p$. Figure 2 shows that there is a first-order correspondence between the two stalagmite $\delta^{18}O$ records but second-order differences between stalagmites in the same cave in the timing and amplitude of the $\delta^{18}O$ series. Comparison with pseudoproxy $\delta^{18}O$ demonstrates that this variability of individual observed stalagmite records is of the same order of magnitude as that modeled. Pseudoproxy *Stal_3*, which has a preferential flow component, has the greatest variability in $\delta^{18}O$ with a consistent 2σ variability of 1.65‰ at 12, 11, and 10 ka. In comparison, *Stal_5*, where waters are derived from the Karst Store 1, has a smaller but nonstationary 2σ variability of 0.36, 0.34, and 0.33‰ at 12, 11, and 10 ka, respectively. We consider this nonstationarity in speleothem $\delta^{18}O$ over time in more detail later in the paper.

[11] First, we consider the magnitude of $\delta^{18}O$ change between the 12, 11, and 10 ka simulations: mean pseudoproxy $\delta^{18}O$ decreases by 0.36‰, whereas the stalagmites decrease by ~1–2‰. This could be attributed to changes in $\delta^{18}O_p$ over time, as this parameter was held constant in the three time-slice input series. We can use the model to investigate the relative importance to stalagmite $\delta^{18}O$ of changes in precipitation intensity and $\delta^{18}O_p$, temperature, and water balance. Our model output demonstrates that with no change in precipitation $\delta^{18}O_p$, a pseudoproxy $\delta^{18}O$ response of -0.36‰ is generated (Figures 1 and 2). This can be attributed to the temperature-dependent fractionation of $\delta^{18}O$ during calcite precipitation (-0.24‰ K^{-1} following *Kim and O'Neil*

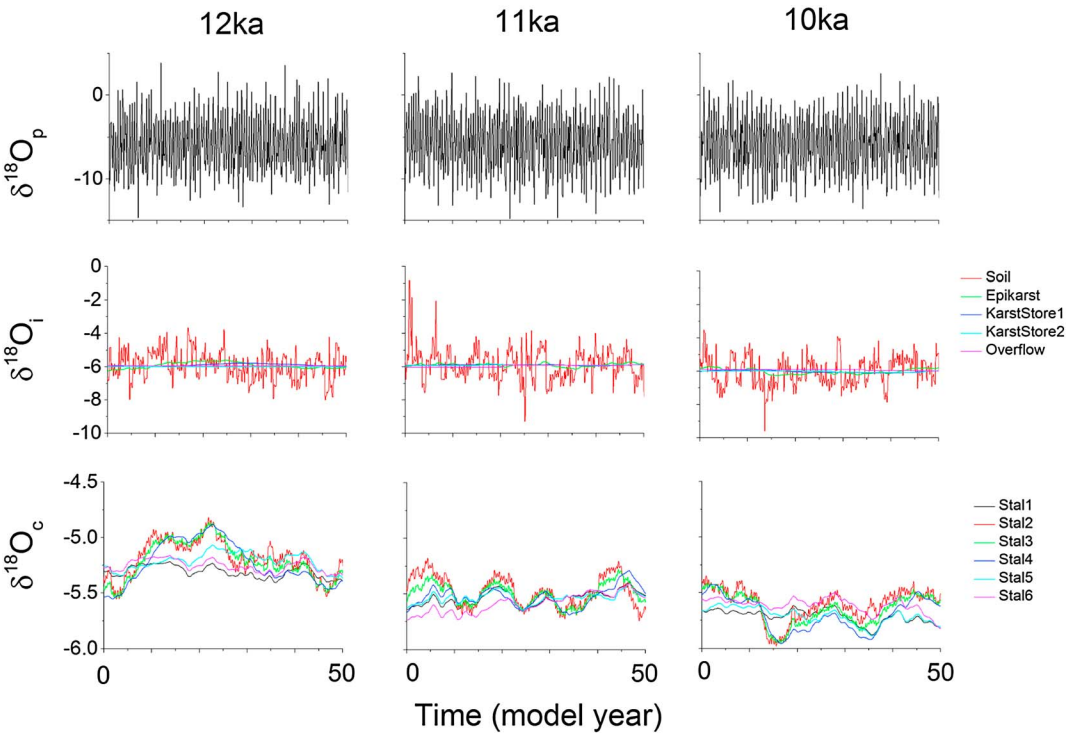

Figure 3. $\Delta\delta^{18}O$ variability from input to pseudoproxy. Comparison of 12, 11, and 10 ka model simulations, using arbitrary 50 year time slices, for steady state parameters of $F3 = 0.008$, $F5 = 0.005$, and $Ovcap = 100$. (top) Precipitation input $\delta^{18}O_p$, (middle) stored infiltration water $\delta^{18}O_i$: Soil Store, Epikarst Store, Karst Store 1, Karst Store 2 and Overflow Store outputs. (bottom) Pseudoproxy series $\delta^{18}O_c$ *Stal_1* to *Stal_6*. Note the different *y* axis scales and the loss of high-frequency variability.

[1997]) between the mean temperature of the 12 and 10 ka time slices (10.5 vs. 12.2°C; using $-0.24‰\ K^{-1}$ would produce a speleothem response of −0.41‰). The influence of changes in precipitation amount and water balance on stalagmite $\delta^{18}O$ over this time period is therefore negligible (~0.05‰ and less than the analytical precision of typical carbonate isotope measurements). This is confirmed in Figure 3, which demonstrates no change in the mean $\delta^{18}O$ of water between soil, epikarst, and karst stores between 12, 11, and 10 ka. For our Chinese example, the highest rainfall occurs in the warmest summer months due to the influence of monsoonal climate conditions (Figure S4 in the supporting information). In theory, cooler glacial conditions and lower *ET* could limit groundwater recharge to summer months (when the soil is not frozen) and, in warmer, postglacial conditions (with higher summer *ET*), recharge could become more evenly distributed through the year. However, input conditions (Figure S4) and model output (Figure 3) demonstrate that summer precipitation is so dominant at 12, 11, and 10 ka that the effects of changes in water balance are negligible in the case of our Chinese example. The change in water balance could become more significant when considering the implications of the larger temperature changes expected over the complete glacial to interglacial transition (3–7°C for warming for T-I (Termination 1) [*Liu et al*., 2012; *Shakun et al*., 2012]) particularly at sites with lower annual *P* and where $P \approx$ PET (for example, semiarid regions, karst regions such as those found in Australia and Arabian Peninsula). Our modeling also demonstrates that changes in *P* amount, such as that arising from an intensification of monsoon intensity, will have little effect on stalagmite $\delta^{18}O$, at least over the 12, 11, and 10 ka time slices (Figure S5). With groundwater recharge dominated by monsoon rain, changes in precipitation intensity have relatively little effect on total recharge and therefore speleothem $\delta^{18}O$.

[12] The combination of general circulation and karst modeling permits the quantification of pseudoproxy $\delta^{18}O$ sensitivity to both *T* and $\delta^{18}O_p$. *T* drives the *T* sensitive fractionation of $\delta^{18}O$ during calcite precipitation (here we use $-0.24‰\ K^{-1}$ following *Kim and O'Neill* [1997]), which would lead to a decrease in speleothem $\delta^{18}O$ of between ~0.7 and ~1.6‰ for the range 3–7°C for warming for T-I. Over the 12 to 10 ka period investigated here, and using a fixed $\delta^{18}O_p$ input series, a decrease in pseudoproxy $\delta^{18}O$ of −0.41‰ can be attributed to the change in *T*, allowing the residual difference between pseudoproxy and actual stalagmite series to be attributed to other factors such as changes in precipitation amount, water balance, and $\delta^{18}O_p$. With the effects of precipitation amount and water balance both negligible for this case study, decreases in mean stalagmite $\delta^{18}O$ of 1.26‰ and 1.53‰ for stalagmites H82 and PD, respectively, between 12.5–12.0 ka and 11.0–10.5 ka can be attributed to changes in $\delta^{18}O_p$ (0.85 to 1.12‰). Our results can be compared to the findings of *Pausata et al*. [2011], who used a fully coupled general circulation model that included abrupt addition of freshwater in to the North Atlantic and off-line isotope-enabled general circulation model to simulate a 1.3‰ change in stalagmite $\delta^{18}O$ at Hulu and attributed 0.9‰ to changes in $\delta^{18}O_p$ and 0.2‰ to changes in precipitation amount for changes in temperature and precipitation of 1.9°C and 4%, respectively.

[13] Our pseudoproxy series also demonstrate variability in $\delta^{18}O$ (the standard deviation of pseudoproxy $\delta^{18}O$ at each

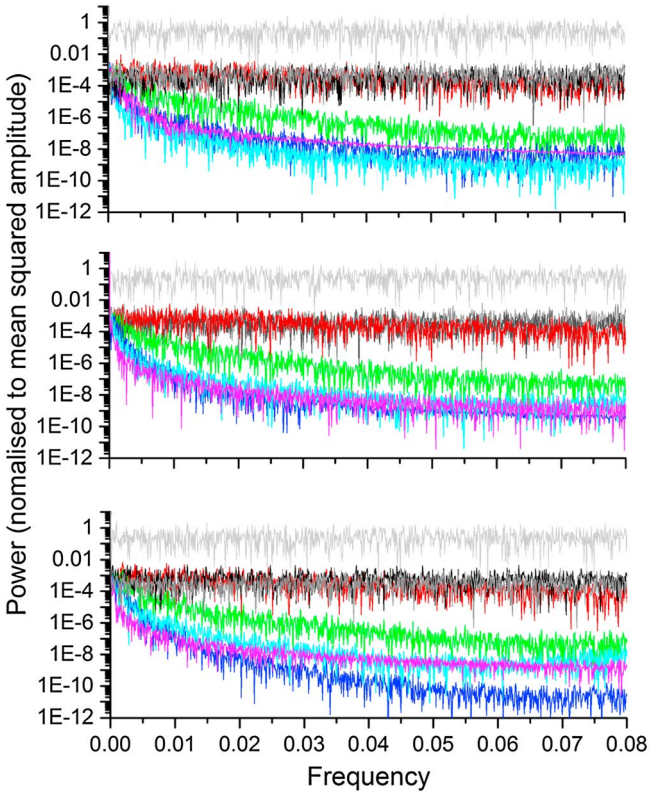

Figure 4. Comparison of fast Fourier transforms of precipitation $\delta^{18}O$ (black), precipitation (light gray), and temperature (dark gray) inputs; Soil Store (red), Epikarst Store (green), Karst Store 1 (blue), Karst Store 2 (cyan), and Overflow Store (magenta). (top) 10 ka, (middle) 11 ka, (bottom) and 10 ka.

time step calculated from all model configurations) that is nonstationary over time and sensitive to model configuration (see Figure S6 in the supporting information). The variability of *Stal_1* and *Stal_6* is higher and more variable than other pseudoproxies. Flow routes associated with both these pseudoproxy series stalagmites, supplied by overflow from Karst Store 2 and the Overflow Store, respectively, are affected by overflow routing and volume of water stored in comparison to specified thresholds (*Ovcap*; *Epicap*). Actual stalagmite $\delta^{18}O$ variability can be expected to increase for model configurations where recharge to these stores becomes discontinuous, albeit at rates that are still sufficient to maintain continuous speleothem deposition. An increase in variability in modeled stalagmite $\delta^{18}O$ is observed from the 12 to 10 ka time slices by the *Stal_2*, *Stal_3*, and *Stal_4* series, although to a lesser extent. All three series receive inflow from the Epikarst Store, with varying proportions of preferential flow. The volume of water stored in the epikarst will decrease due to increased *ET*, as shown in Figure S4, which in turn leads to increased pseudoproxy $\delta^{18}O$ variability.

[14] It is also interesting to note that the pseudoproxy series in Figures 1 and 3 only preserve low-frequency, decadal-scale variability. This is demonstrated in the spectral analyses presented in Figure 4. Inspection of model output demonstrates that this loss of high-frequency, annual-scale variability originates in the model, predominantly in the epikarst and karst stores (see Figure 3). It is only in the soil store where the $\delta^{18}O$ of high recharge events can significantly affect the overall store isotope composition. Isotope variability can therefore be introduced in this store as a result of recharge events where $P >> ET$, store volume is low in the preceding time step, and the isotopic composition of event water is significantly different from the mean. However, when subsequently mixed with other karst stores, this high-frequency variability is smoothed, and only low-frequency periodicity remains in the speleothem $\delta^{18}O$ record. This finding has two important implications: (1) where high-frequency variation of $\delta^{18}O$ is observed in speleothems, a karst modeling approach can be used to determine whether this can be attributed to internal cave processes (e.g., kinetic fractionation) or is a climate signal (e.g., in the case of tropical cyclones, where high recharge events of distinct isotope composition may occur [*Frappier et al.*, 2007]); (2) that any low-frequency signal contained in speleothem $\delta^{18}O$ is likely to be modulated by the interplay between *P*, *ET*, and the properties of the soil store.

4. Conclusions

[15] Our hydrological modeling approach has permitted a quantitative assessment of the relative importance of changes in the temperature, precipitation, and water balance and specifically the timing and amount of groundwater recharge on stalagmite $\delta^{18}O$ over glacial transitions. The pseudoproxy series demonstrate the extent to which variability between published stalagmite $\delta^{18}O$ records can be specifically attributed to hydrological variability. Importantly, it demonstrates that "wiggle matching" of stalagmite $\delta^{18}O$ series should not be attempted, at least over decadal-centennial time scales, particularly where stalagmite $\delta^{18}O$ variability is similar to that which can be ascribed to hydrological variability. This finding is likely to be generally applicable to all stalagmite $\delta^{18}O$ records, although the absolute hydrological uncertainty will vary on a site-by-site basis.

[16] We identify nonstationarity in pseudoproxy $\delta^{18}O$ variability that is a response to changing water balance and its effects on karst aquifer storage. This demonstrates that changes in stalagmite $\delta^{18}O$ variability over time cannot be simply attributed to changes in any single climate parameter, given the extent to which groundwater storage and flux are sensitive to the water balance. We demonstrate the importance of considering the water balance, which although not affecting pseudoproxy $\delta^{18}O$ over the 12 to 10 ka period would be expected to be a factor in determining stalagmite $\delta^{18}O$ during periods of significant ΔT (e.g., over glacial terminations). The water balance would also be expected to affect stalagmite $\delta^{18}O$ for lower values of ΔT in regions where recharge is more sensitive to *ET*. Further research is needed to quantify the importance of this process.

[17] Finally, our pseudoproxy series lose high-frequency power and contain only low-frequency information. Our results demonstrate that this signal transformation arises from the soil store through changes in the water balance, with the $\delta^{18}O$ of high recharge ($P >> ET$) events modulating the mean soil store $\delta^{18}O$ composition and volume. For speleothem samples whose recharge is dominated by the properties of this store (such as our pseudoproxies *Stal_2* and *Stal_3*) this may yield high-frequency $\delta^{18}O$ records of high-recharge events. However, for speleothem $\delta^{18}O$ series with significant karst storage (such as those represented by pseudoproxies *Stal_1* and *Stal_5*), the extent to which low-frequency information at decadal to centennial time scales demonstrates periodicity,

which is climatically driven as opposed to an amplification of soil storage properties, requires further research.

[18] **Acknowledgments.** We would like to thank our presubmission reviewers, Joshua Larsen, Adam Hartland, Charlotte Cook, and Bryce Kelly and the comments of two anonymous reviewers.

[19] The Editor thanks 2 anonymous reviewers for their assistance in evaluating this paper.

References

Baker, A., C. Bradley, S. Phipps, M. Fischer, I. J. Fairchild, L. Fuller, C. Spötl, and C. Azcurra (2012), Millennial-scale forward models and pseudoproxies of stalagmite $\delta^{18}O$: An example from NW Scotland, *Clim. Past*, *8*, 1153–1167, doi:10.5194/cp-8-1153-2012.

Bradley, C., A. Baker, C. Jex, and M. J. Leng (2010), Hydrological uncertainties in the modelling of cave drip-water $\delta^{18}O$ and the implications for stalagmite palaeoclimate reconstructions, *Quat. Sci. Rev.*, *29*, 2201–2214, doi:10.1016/j.quascirev.2010.05.017.

Chen, D., G. Gao, C.-Y. Xu, J. Guo, and G. Ren (2005), Comparison of the Thornthwaite method and pan data with the standard Penman-Monteith estimates of reference evapotranspiration in China, *Clim. Res.*, *28*, 123–132, doi:10.3354/cr028123.

Cheng, H., R. L. Edwards, W. S. Broecker, G. H. Denton, X. King, Y. Wang, R. Zhang, and X. Wang (2009), Ice age terminations, *Science*, *326*, 248–252, doi:10.1126/science.1177840.

Cheng, H., P. Z. Zhang, C. Spotl, R. L. Edwards, Y. J. Cai, D. Z. Zhang, W. C. Sang, M. Tan, and Z. S. An (2012), The climatic cyclicity in semiarid-arid central Asia over the past 500,000 years, *Geophys. Res. Lett.*, *39*, L01705, doi:10.1029/2011GL050202.

Dayem, K. E., P. Molnar, D. S. Battisti, and G. H. Roae (2010), Lessons learned from oxygen isotopes in modern precipitation applied to interpretation of speleothem records of paleoclimate from eastern Asia, *Earth Planet. Sci. Lett.*, *295*, 219–230, doi:10.1016/j.epsl.2010.04.003.

Frappier, A. B., D. Sahagian, S. J. Carpenter, L. A. González, and B. R. Frappier (2007), Stalagmite stable isotope record of recent tropical cyclone events, *Geology*, *35*, 111–114.

Kim, S. T., and J. R. O'Neil (1997), Equilibrium and nonequilibrium oxygen isotope effects in synthetic carbonates, *Geochim. Cosmochim. Acta*, *61*, 3461–3475, doi:10.1016/S0016-7037(97)00169-5.

Liu, Z, et al. (2012), Younger Dryas cooling and the Greenland climate response to CO_2, *Procs. Nat. Acad. Sci.*, doi:10.1073/pnas.1202183109.

Pausata, F. S. R., D. S. Battisti, K. H. Nisancioglu, and C. M. Bitz (2011), Chinese stalagmite $\delta^{18}O$ controlled by changes in the Indian monsoon during a simulated Heinrich event, *Nat. Geosci.*, *4*, 474–480, doi:10.1038/NGEO1169.

Peltier, W. R. (2004), Global glacial isostasy and the surface of the Ice-Age Earth: The ICE-5G (VM2) Model and GRACE, *Ann. Rev. Earth. Planet. Sci.*, *32*, 111–149.

Phipps, S. J., L. D. Rotstayn, H. B. Gordon, J. L. Roberts, A. C. Hirst, and W. F. Budd (2011), The CSIRO Mk3L climate system model version 1.0—Part 1: Description and evaluation, *Geosci. Model. Dev.*, *4*, 483–509, doi:10.5194/gmd-4-483-2011.

Phipps, S. J., L. D. Rotstayn, H. B. Gordon, J. L. Roberts, A. C. Hirst, and W. F. Budd (2012), The CSIRO Mk3L climate system model version 1.0—Part 2: Response to external forcings, *Geosci. Model. Dev.*, *5*, 649–682, doi:10.5194/gmd-5-649-2012.

Scholz, D., C. Mühlinghaus, and A. Mangini (2009), Modelling $\delta^{13}C$ and $\delta^{18}O$ in the solution layer on stalagmite surfaces, *Geochim. Cosmochim. Acta*, *73*, 2592–2602, doi:10.1016/ j.gca.2009.02.015.

Shakun, J. D., P. U. Clark, F. He, S. A. Marcott, A. C. Mix, Z. Liu, B. Otto-Bliesner, A. Schmittner, and E. Bard (2012), Global warming preceded by increasing carbon dioxide concentrations during the last deglaciation, *Nature*, *484*, 49–55, doi:10.1038/ nature10915.

Thornthwaite, C. W. (1948), An approach toward a rational classification of climate, *Geog. Rev.*, *38*, 55–94.

Wang, Y. J., H. Cheng, R. L. Edwards, Z. S. An, J. Y. Wu, C.-C. Shen, and J. A. Dorale (2001), A high resolution absolute dated late Pleistocene monsoon record from Hulu Cave, China, *Science*, *294*, 2345–2348, doi:10.1126/science.1064618.

Wang, Y., H. Cheng, R.-L. Edwards, X. Kong, X. Shao, S. Chen, J. Wu, X. Jiang, X. Wang, and Z. An (2008), Millennial- and orbital-scale changes in the East Asian monsoon over the past 224,000 years, *Nature*, *451*, 1090–1093, doi:10.1038/nature06692.